J. Phys. IV France **112** (2003)
© EDP Sciences, Les Ulis
DOI: 10.1051/jp4:2003851

The kinetics of lath martensitic transformation

G. Ghosh and G.B. Olson

Department of Materials Science and Engineering, Robert R. McCormick School of Engineering and Applied Science, Northwestern University, 2225 N. Campus Drive, Evanston, IL 60208-3108, U.S.A.

Abstract. The multicomponent solution thermodynamics, a model for barrierless heterogeneous martensitic nucleation, a model for the composition and temperature dependence of the shear modulus, and a set of unique interfacial kinetic parameters are integrated to model the kinetics of lath martensitic transformation. It is shown that M_S in multicomponent alloys can be predicted within ±40K. The geometric partitioning of austenite grain and the dependence of average lath volume on the fraction transformed is established by a careful analysis of lath microstructure. The main contribution of lath martensitic transformation is due to autocatalytically generated defects.

1. INTRODUCTION

The kinetics of martensitic transformation is of significant scientific and technological interest. Mechanistic models to predict the lath martensitic transformation kinetics are needed to design new alloys in composition ranges previously unexplored [1]. To assist the science-based design of alloys with lath martensitic microstructure in Fe-base alloys, we have developed models to predict both the martensitic start temperature (M_s) and the overall transformation kinetics. As presented below, this is done by integrating computational thermodynamics, a model for the composition and temperature dependence of shear modulus of austenite, a model for heterogeneous martensitic nucleation, and the phenomenological model for the transformation kinetics.

2. COMPUTATIONAL THERMODYNAMICS AND THE DRIVING FORCE CALCULATION

Martensitic transformations can be regarded as a form of spontaneous plastic deformation driven by chemical forces [2]. Due to the virtually diffusionless nature of the fcc->bcc martensitic transformation in Fe-base alloys, the molar chemical driving force (ΔG_{ch}) at a constant temperature and pressure is given by

$$\Delta G_{ch} = G_m^{\alpha} - G_m^{\gamma} \tag{1}$$

where G_m^{α} and G_m^{γ} are the molar Gibbs energies bcc(α) and fcc(γ) phases, respectively. Using Thermo-Calc software systems [3], we have developed a multicomponent thermodynamic database to calculate ΔG_{ch}. Some of the salient features of this database have been discussed elsewhere [4].

3. THE CRITICAL DRIVING FORCE FOR FCC -> BCC MARTENSITIC NUCLEATION

The heterogeneous nature of fcc –> bcc martensitic nucleation is well established for both bulk materials and small particles [1]. In the dislocation dissociation mechanism for martensitic nucleation [2], the critical condition for semicoherent nucleation is given by a balance between the negative fault energy and the interfacial frictional work. The critical driving force needed for barrierless nucleation from a defect of potency n (defined by the number of closed packed planes) is expressed as

$$\Delta g_{ch}(n) = -\left[g^{el} + \frac{2\sigma}{nd} + w_{\mu} + w_{th} + w_{\rho} \right] \tag{2}$$

where Δg_{ch} is the driving force per unit volume, n is the thickness of the critical nucleus stabilized by the defect interaction and it is measured in units of interplanar spacing d of closest packed planes, g^{el} is the shape insensitive component of the strain energy (per unit volume) associated with distortions in the nucleus habit plane, σ is the semicoherent interfacial energy, w_{μ} and w_{th} are the athermal and thermal components of the interfacial frictional work due to solute atoms, respectively, and w_{ρ} is the interfacial frictional work due to dislocation forest (primarily athermal). In annealed materials and if the M_s temperature is sufficiently high, w_{th} and w_{ρ} are considered to be negligible at M_s. To evaluate g^{el}, σ, w_{μ} *etc*, an important material property is the composition and temperature dependence of isotropic shear modulus of austenite [4].

Very recently, we have a developed a model to predict the composition and temperature dependence of isotropic shear modulus (μ) of austenite [5]. The temperature dependence of μ of pure γ-Fe ($\mu_{\gamma\text{-Fe}}$) as [5]

$$\mu_{\gamma-Fe} = 9.2648[1 - 7.9921\mathbf{x}10^{-7}T^2 + 3.3171\mathbf{x}10^{-10}T^3]\text{x}10^{10}\ \text{N/m}^2 \tag{3}$$

where T is the temperature in K. For the multicomponent fcc solid solutions, we propose the following relation incorporating the linear superposition effect of the alloying elements

$$\mu_{\gamma-Fe} = \left(9.2648 + \Sigma x_j \left(\frac{d\mu}{dx_j} \right) \right)[1 - 7.9921\text{x}10^{-7}T^2 + 3.317\text{x}10^{-10}T^3]\text{x}10^{10}\ \text{N/m}^2 \tag{4}$$

where the constant term is the shear modulus of *paramagnetic* γ-Fe at 0 K, and x_j is the mole fraction of element j. Table 1 lists dμ/dx for the alloying elements of interest.

Table 1. The effect of alloying elements on the isotropic shear modulus (dμ/dx, x10^{10} N/m^2) of γ-Fe [5].

Al	C	Co	Cr	Cu	Mn	Mo	N	Nb	Ni	Si	Ti	V	W
-27.741	-10.889	-2.024	-0.738	10.423	-2.675	2.940	-12.313	-9.241	-6.049	-14.914	-11.169	2.350	8.196

The temperature dependence of strain energy g^{el} scales with the temperature dependence of the isotropic shear modulus of austenite. The primary contribution to the semicoherent interfacial energy is the elastic energy associated with the short range stresses (due to local deviation from the invariant plane strain condition) near the interface. Since the dislocation self-energy is proportional to the shear modulus, the interfacial energy scales with the shear modulus. Therefore, for multicomponent alloys we propose

$$g^{el} = K^{el}\mu(x_j, T) \tag{5a}$$

$$\sigma = K^{\sigma}\mu(x_j, T) \tag{5b}$$

where $\mu(x_j, T)$ denotes the composition (x_i) and temperature dependence of shear modulus of austenite. The constants K^{el} and K^{σ} in Eqs. 5(a) and 5(b) are evaluated as 9.4x10^{-4} and 2.2077x10^{-12} m.

In metallic alloys, interactions of solute atoms, defect clusters and dislocation forests with the martensitic interface long-range stress field give rise to an athermal resisting force while interactions with the interfacial core give rise to short-range contributions that can be overcome by thermal activation. Depending on the microstructural element, these interactions can be point-line, point-surface, line-line, line-surface and surface-surface types. Accordingly, the athermal resisting force is also expected to scale with the temperature dependent shear modulus. Accordingly, for multicomponent alloys we propose

$$w_{\mu} = A_{\mu}\mu(x_i, T) \tag{6a}$$

$$A_\mu = \sqrt{\Sigma(K_\mu^i x_i^{0.5})^2} + \sqrt{\Sigma(K_\mu^j x_j^{0.5})^2} \quad (6b)$$

where i = Al, C, N, Cr, Mn, Mo, Nb, Si, Ti, V, W, and j = Co, Cu, Ni. Based on the evaluated K_μs listed in Table 2, we have divided the solute elements into two distinct categories of relative obstacle strength in which each category represents solutes of similar strengths and a linear superposition between the categories representing the solutes of very different strengths. An earlier interpretation of effect of Co on M_s was to reduce the shear modulus [6] of γ-Fe; however, our recent modeling of the composition dependence of shear modulus suggests that this is not so. The true reason why Co raises M_s is its effect on thermodynamics.

Table 2. The modulus-normalized coefficients (K_μ) representing the athermal friction of different solutes for the fcc/bcc martensitic interface in Eq. (6b).

Al	C	Co	Cr	Cu	Mn	Mo	N	Nb	Ni	Si	Ti	V	W
0.00262	0.01012	0.00015	0.00435	0.00139	0.00475	0.00321	0.00818	0.00285	0.00043	0.00386	0.00305	0.00243	0.00325

3.1. The Prediction of M_s of Multicomponent Alloys

Figure 1 shows a comparison between the experimental [7] and predicted M_s temperatures for some commercial alloys. In the context of martensitic transformation in multicomponent alloys, it is necessary to ascertain the composition of austenite that undergoes martensitic transformation upon quenching from high temperature. In predicting the M_s temperatures of the alloys in Fig. 1, the austenite composition was taken to be that obtained from the calculated phase equilibria [4] at the reported solution treatment temperatures using the SSOL database of the Thermo-Calc software [3]. The agreement between the predicted M_s and the experimental M_s in Fig. 1 is good if we assume an uncertainty of ±40 K for the experimental data. Also, the level of agreement between the predicted and experimental M_s is the same, irrespective of whether the alloy is single phase or polyphase at the solution treatment temperature T_s.

4. THE OVERALL TRANSFORMATION KINETICS

Figure 2 shows the overall transformation curves for three multicomponent alloys that exhibit a lath martensitic microstructure. Typically, these athermal transformation curves have three regions: (i) just below M_s, a narrow temperature range where the transformation rate (df/dT) is constant (f = fraction martensite), (ii) a temperature range where the df/dT increases with decreasing temperature due to the dominance of autocatalysis, and (iii) a temperature range where df/dT decreases with decreasing temperature due to the dominance of geometric partitioning when the austenite is divided into numerous tiny compartments. In conjunction with the phenomenological model developed for isothermal martensitic transformation, the athermal transformation curves can be used to derive the autocatalytic factor associated with lath martensite if the average volume ($\overline{V}$) of lath as a function of f is known.

Figure 3 is a micrograph of lath martensite showing that a prior austenite grain consists of many packets (numbered) within which the laths are arranged in a parallel manner. In addition, several laths which have nucleated at a prior austenite grain boundary (marked with arrows) may also be seen. Generally, the grain boundary laths are much bigger than those constitute the packets. Dividing the austenite grains into many packets (according to the arrangement of the laths) and assuming the volume of lath within each packet is constant, we have established the $\overline{V}$ vs f relationship.

For a first-order martensitic transformation, f is given by the product of $\overline{V}$ and total number of nuclei (N_t). The parameter N_t at any temperature per unit volume of alloy can be described as

$$N_t = (N_i + Pf - N_v)(1 - f) \quad (7)$$

where N_i is the number of preexisting nucleation sites in the parent phase, P is the autocatalytic nucleation sites produced per unit volume of martensite formed, and N_v is the number of laths formed per unit volume of alloy. Knowing ΔG_{ch} as a function of temperature and the $\overline{V}$ vs. f relationship, it is possible to derive

P from Eq. (7). Figure 4 compares the intial defect density ($N_i(n)$) and P as function of defect potency (n) for lath martensite. It is seen that P for lath martensite is 4 to 10 orders of magnitude larger than $N_i(n)$. This implies that the initial defects contribute very little to the overall lath martensitic transformation, and the main contribution is due to autocatalytically generated defects. Furthermore, we find that the magnitude of P for lath martensite is about 4 orders higher than the plate martensite [8].

Acknowledgments

This work was supported by the National Science Foundation under Grant No. DMR-9806749.

References

[1] Ghosh G. and Olson G.B., *Acta Metall. Mater.*, **42** (1994) 3361-3370.
[2] Olson G.B. and Cohen M., "Dislocation Theory of Martensitic Transformations", Dislocations in Solids, edited by F.R.N. Nabarro (North Holland, Amsterdam, 1986), **Vol. 7**, pp.297-407.
[3] Sundman B., Jansson B. and Andersson J.O., *CALPHAD*, **9** (1985) 153-190.
[4] Ghosh G. and Olson G.B., *J. Phase Equilibria*, **22** (2001) 203-207.
[5] Ghosh G. and Olson G.B., *Acta Mater.*, **50** (2002) 2655-2675.
[6] Goldman A.J. and Robertson W.D., *Acta Metall.*, **12** (1964) 1265-1275.
[7] Atlas for Time-Temperature Diagrams for Iron and Steels, edited by G.F. Vander Voort (ASM International, Materials Park, OH, 1991).
[8] Lin M., Olson G.B. and Cohen M., *Metall. Trans. A*, **23A** (1992) 2987-2998.

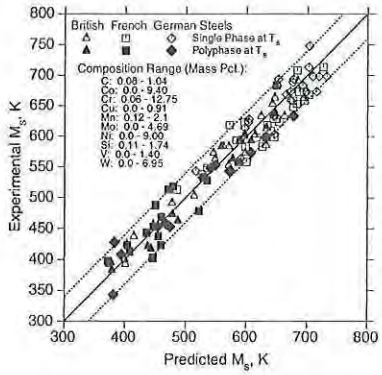

Figure 1. Comparison between the experimental and calculated M_s temperatures of multicomponent alloys.

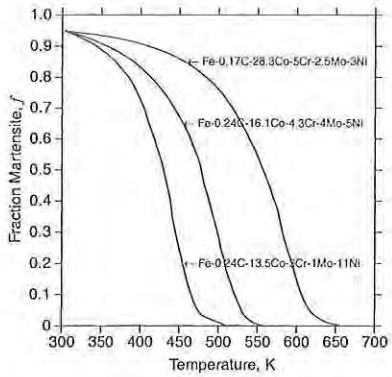

Figure 2. Athermal transformation curves of three alloys having lath martesite microstructure.

Figure 3. Lath microstructure of an Fe-0.16C-14.3Co-2.1Cr-1Mo-10.2Ni alloy (M_s=573K).

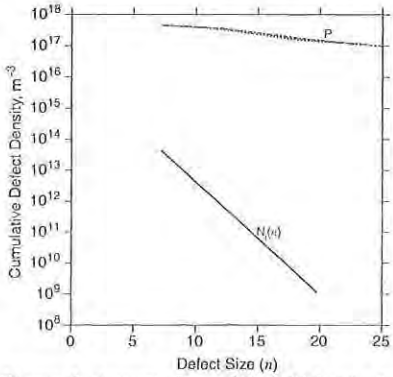

Figure 4. A comparison of the initial and autocatalyitc defect distribution associated with lath martensite microstructure.